“Feathered” fractal surfaces to minimize secondary electron emission for a wide range of incident angles

Charles Swanson, and Igor D. Kaganovich

Citation: Journal of Applied Physics **122**, 043301 (2017);
View online: https://doi.org/10.1063/1.4995535
View Table of Contents: http://aip.scitation.org/toc/jap/122/4
Published by the American Institute of Physics

"Feathered" fractal surfaces to minimize secondary electron emission for a wide range of incident angles

Charles Swanson and Igor D. Kaganovich
Princeton Plasma Physics Laboratory, Princeton University, Princeton, New Jersey 08543, USA

(Received 3 April 2017; accepted 11 July 2017; published online 24 July 2017)

Complex structures on a material surface can significantly reduce the total secondary electron emission from that surface. The reduction occurs due to the capture of low-energy, true secondary electrons emitted at one point of the structure and intersecting another. We performed Monte Carlo calculations to demonstrate that fractal surfaces can reduce net secondary electron emission produced by the surface as compared to the flat surface. Specifically, we describe one surface, a "feathered" surface, which reduces the secondary electron emission yield more effectively than other previously considered configurations. Specifically, feathers grown onto a surface suppress secondary electron emission from shallow angles of incidence more effectively than velvet. We find that, for the surface simulated, secondary electron emission yield remains below 20% of its unsuppressed value, even for shallow incident angles, where the velvet-only surface gives reduction factor of only 50%. *Published by AIP Publishing*. [http://dx.doi.org/10.1063/1.4995535]

I. INTRODUCTION

Secondary electron emission (SEE) from dielectric and conductive surfaces can significantly change the flux and potential profiles at material interfaces, often limiting the performance of many plasma applications and vacuum electronics such as RF amplifiers,[1] particle accelerators, and Hall thrusters.[2–4] For these applications, it is important to reduce the flux of secondary electrons emitted from the surface. Various textures and treatments have been applied to material surfaces to minimize this secondary electron emission, such as triangular grooves,[5–8] oxides,[9] fibrous structures (velvet, fuzz, and foam[4,10–14]), and dendritic structures.[15] Ye *et al.* have recently analyzed and optimized a micro-porous surface to minimize SEE.[16] However, the search for practical solutions for surfaces that can extinguish secondary electron emission is still continuing, and we demonstrate that fractal, feathered surfaces are promising candidates. In this paper, "reduced by $n\%$" means $\gamma \rightarrow \left(1 - \frac{n}{100\%}\gamma\right)$ and "reduction factor $n\%$" means $\gamma \rightarrow \frac{n}{100\%}\gamma$.

II. GEOMETRIC CONSIDERATION

Consider a flat surface with some secondary electron emission yield (SEY, the ratio of secondary electron flux to primary electron flux) γ_{flat}. Now suppose there is some texture that can be applied to the surface to produce a reduced secondary electron emission yield, $\gamma = R\gamma_{flat}$, where $R < 1$.

Some examples of such textures are, as noted in Sec. II, triangular grooves,[5–8] velvet and other fibers,[4,10–14] and dendritic structures.[15] The mechanism for SEY suppression is the capture of first-generation secondary electrons emitted from deep inside the structure. In order to contribute to the net outgoing secondary electron emission flux, electrons must traverse this structure without intersecting any part of it and escape.

If this surface is continuous, we can consider a zoomed-in system of one surface element which appears flat. If this flat surface is textured again with smaller-scale versions of the surface, then an electron will have to traverse both the primary structure at the initial scale and the secondary structure at the smaller scale. Thus, the reduction factor R can be reduced further to some smaller $R_{new} = R \cdot R_1$.

This argument implies that if we continue this process N times and create an Nth-order geometry, which is a geometry that has had smaller versions of itself tiled onto its flat surface elements at N different smaller scales, it will be a suitable surface to greatly reduce the SEY from a flat surface.

Surfaces produced by this procedure will look self-similar at all scales. If the seed geometry is a triangular groove, for example, the recursed geometry is the Koch curve.[17] If $N \rightarrow \infty$, such a surface is a fractal.

It is not necessarily the case that $R_1 = R$. The numerical value of R is calculated by averaging over angular distribution of the emitted secondary electrons. For a flat surface, this distribution is assumed to follow a cosine law.[18] However, this assumption does not hold for the fractal surface. The angular distribution of emitted secondary electrons from a complex surface can be strongly non-cosine at large distances from a small-scale structure due to geometrical consideration of the view angle. Therefore, the SEY reduction factor for an Nth order recursion of geometry down to smaller scales does not necessarily scale as R^N.

III. VELVET AS A CHOICE FOR THE SEED GEOMETRY

If the seed geometry is a velvet surface, which is a lattice of long whiskers grown onto a flat substrate, the recursed geometry will be a lattice of whiskers which themselves have whiskers grown onto their sides, like down-feathers, as shown in Fig. 1. We refer to this surface as a "feathered" surface for this reason.

The reduction in SEY from a velvet surface was studied in our previous paper.[13] Velvet is most efficient at reducing SEY for electron flux normal to the surface, for $\theta \approx 0$, θ

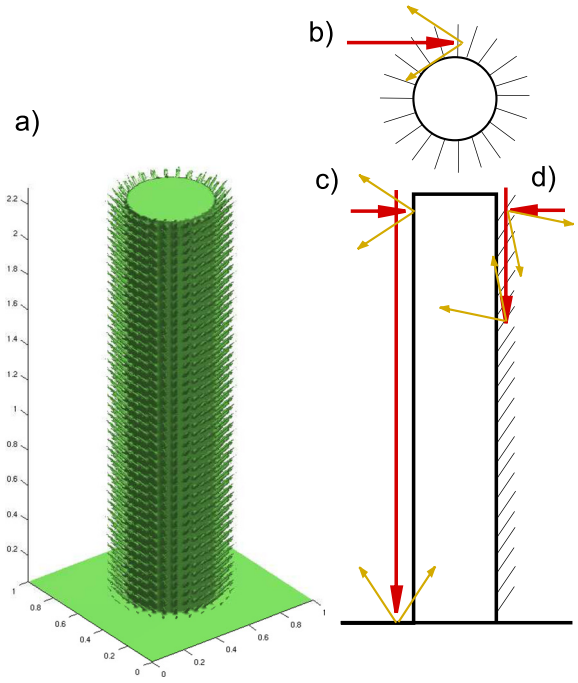

FIG. 1. (a) Drawing of the "whisker on a whisker" geometry and schematic representations of the suppression mechanism. This geometry corresponds to a shorter, fatter ($D = 16\%, A = 10$ rather than $D = 4\%, A = 80$) geometry than the one calculated. At right are shown the effects described in Sec. VI: (b) increase in effective capture area. (c) Normal and shallow incident primary electrons on a velvet geometry. (d) Normal and shallow incident primary electrons on a feathered geometry. Red arrows correspond to primary electron trajectories. Yellow arrows correspond to example secondary electron trajectories.

being the polar angle between normal to the surface and velocity of the incident primary electrons. The most efficient reduction is predicted for the velvet with rarely spaced long whiskers. The necessary condition for maximum reduction in the SEY can be expressed as requirement for the dimensionless parameter

$$u \equiv \frac{2}{\pi} DA \gg 1, \tag{1}$$

where A is the aspect ratio, $A = h/r \gg 1$, h is the whisker height and r is the whisker radius, D is the whisker packing density, $D = \pi r^2/s^2 \to 0$, and s is the inter-whisker spacing.

When this condition is met, the reduction factor in SEY can be smaller than 0.1 for normal incidence $\theta \approx 0$.

However, velvet cannot significantly reduce SEY for shallow incident angles. A reduction factor of SEY, R, for velvet is shown in Fig. 2 for the line labeled "Primary whiskers, $u = 2, 4, \infty$." The SEY reduction factor is maximum for a shallow incident primary angles $\theta \approx 90^\circ$, where $R \simeq 0.5$. The results can be explained as follows: For $\theta \approx 90^\circ$, the impinging primary electrons hit the whiskers near their tops, and secondary electrons are either emitted in the upward hemisphere or downward hemisphere with equal probability. Electrons emitted in the upward hemisphere escape, whereas in the downward hemisphere intersect velvet and do not escape. Hence, $R \simeq 0.5$ for $\theta \approx 90^\circ$.

Modification of a velvet surface to a feathered surface is needed to overcome this limitation in SEY reduction for

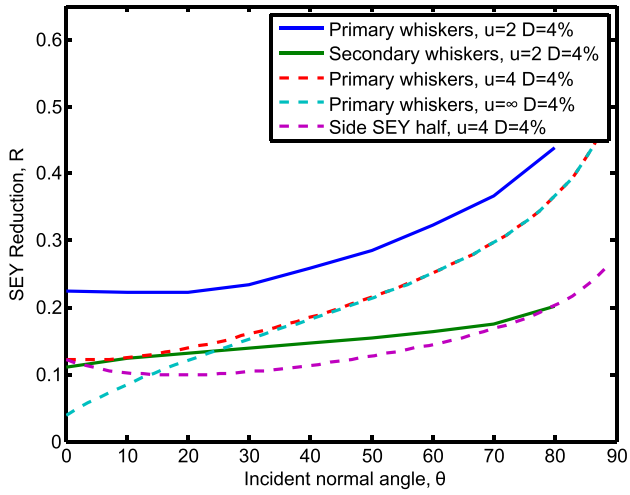

FIG. 2. Solid lines show the result of the numerical Monte Carlo calculation: reduction in SEY of the considered $u = 2$ graphite velvet either without another recursive velvet grown onto the whisker sides ("Primary whiskers, $u = 2$") or with this smaller velvet ("Secondary whiskers, $u = 2$"). Also shown (2 dashed lines) are the result of the analytic model in our previous paper[13] for the case of velvet with $u = 4$ and $u = \infty$ for velvets with $D = 4\%$. Also shown (last dashed line) is the result of the analytic model for $u = 4, D = 4\%$, but with the emission from the sides of the whisker reduced by half.

shallow angles. Regarding processes that can yield feather-like structures, volumetric chemical processes have been identified, which do cause velvet-like, fractal-like shapes to self-generate.[19] The same chemical processes that grow large-diameter velvet onto the flat substrate may also be used to grow small-diameter velvet onto the sides of large-diameter velvet.

IV. MONTE CARLO CALCULATIONS OF SECONDARY ELECTRON EMISSION YIELD

We performed a Monte Carlo calculation of the SEY of feathered surface. We used the same simulation tool that was previously used to simulate SEY of the velvet and was benchmarked against analytical calculations.[13]

We simulated two surfaces: a velvet and a feathered surface, that is, velvet with one recursion, that is, a velvet surface onto whose whisker sides many, smaller whiskers were placed. An example of the feathered geometry is depicted in Fig. 1. We found that the results were improved (R is smaller) if the secondary whiskers are placed at a 45° angle upward, rather than downward or straight-out normal to the whisker surface.

The velvet parameters that we used for this calculation were as follows: the packing density $D = 0.04$ and the aspect ratio $A = 80$, which correspond to a dimensionless parameter $u = \frac{2}{\pi} AD = 2$. For these parameters, a reduction of $0.2 < R < 0.5$ is expected for velvet. The small whiskers that were placed onto the sides of the big whiskers were $80\times$ smaller. They have the same $D = 4\%$, with $A = 80 \cdot \sqrt{2}$, and were pointed upward at a 45° angle. Note that the radial extent of the secondary whiskers is therefore equal to the radius of the primary whiskers.

We numerically simulated the emission of secondary electrons by using the Monte Carlo method, initializing

many particles and allowing them to follow ballistic, straight-line trajectories until they interact with the surface. The surface geometry was implemented as an isosurface, a specially designed function of space that gives correct feathered structure. The SEY of a particle interacting with a flat surface was assumed to follow the empirical model of Scholtz[20]

$$\gamma(E_p,\theta)=\gamma_{max}(\theta)\times\exp\left[-\left(\frac{\ln\left[E_p/E_{max}(\theta)\right]}{\sqrt{2}\sigma}\right)^2\right]. \quad (2)$$

For parameters in the model $\gamma_{max}(\theta)$, E_p, $E_{max}(\theta)$, σ, we used those of graphite,[13] assuming the structures are carbon based. We initialized the primary electrons with energy of 50 eV, 200 eV, or 1000 eV. True secondary electrons, elastically scattered electrons, and inelastically scattered electrons were taken into consideration. At this energy, 2.3% of secondary electrons are elastically scattered according to our model. For more discussion on the model and its implementation in the Monte Carlo calculations, see our previous paper on SEE from velvet.[13]

V. SEY OF THE FEATHERED SURFACE AS COMPARED TO THE VELVET

The SEY reduction factor as a function of primary angle of incidence θ and several values of parameter u are depicted in Fig. 2. These simulations were performed for 200 eV primary electrons. The blue solid line, "Primary whiskers, $u=2$," shows the SEY from the primary velvet described in Sec. V ($D=4\%$, $A=80$). The SEY reduction factor for this case is between $R=0.2$ for $\theta\approx 0$ and $R=0.4$ for $\theta\approx 90^\circ$. The green solid line, "Secondary whiskers, $u=2$," shows the SEY from the feathered structure described in Sec. V (primary whiskers: $D=4\%$, $A=80$; secondary whiskers: $D=4\%, A=80\cdot\sqrt{2}$, $80\times$ smaller and pointed upward at a 45° angle). It is apparent that adding whiskers to the sides of the primary whiskers reduces the SEY dramatically for every θ.

The dashed lines are the result of an analytic model described in our previous paper.[13] The first two dashed lines (red and cyan) correspond to $D=4\%, A=160$, $u=4$ and $D=4\%$, $A=\infty$, respectively.

The last, magenta line titled, "Side SEY half," shows the analytical result for SEY for the $D=4\%$, $A=160$ case, but with the SEY from the sides of the whiskers reduced by half. Our previous paper gives expressions for the contribution to the SEY from the tops and sides of the velvet whiskers and the bottom surface, $\gamma=\gamma_{tops}+\gamma_{sides}+\gamma_{bottom}$. The result, "Side SEY half," was obtained assuming the SEY from the sides of the primary velvet whisker is reduced by one half due to the addition of the secondary whiskers, $\gamma_{sides}\rightarrow 1/2\cdot\gamma_{sides}$.

The result for $u=4$ is included to compare SEY for the feathered structure with the velvet with the larger radius because the addition of whiskers extending outward from the primary whiskers increases the effective radius, increasing the capture cross section and capturing electrons that may otherwise have escaped (see Fig. 1). From Fig. 2, it is apparent that this effect is sufficient to explain the improvement in SEY of the feathered geometry at normal incidence, $\theta\approx 0$, because red dashed line coincides with the green line.

Simply increasing the radius of the primary whisker by this amount would increase D to 16% (and decrease A to 40, and increase u to 4). This increases the number of electrons that are emitted from the tops and escape. Figure 1(d) shows that this larger D effect is not the case when the effective extra radius is made up of secondary whiskers; instead, the secondary electrons are directed inward and are captured by the structure.

The result for $u=4$ with the SEY from the sides of the whisker reduced by half is included to explain the other interesting observation for shallow incidence angles ($\theta\approx 90^\circ$) that shows SEY reduction in the feathered case. Indeed, the feathered geometry even out-performs an infinitely long velvet case, that of $u=\infty$ in this regime. This is because, as depicted in Fig. 1(c), when the primary incidence angle is shallow, primary electrons hit velvet whiskers very close to their tops, and nearly half of the secondary electrons are emitted with velocity in the upward direction and escape. As depicted in Fig. 1(d), primary electrons incident with shallow angles hit feathered whiskers very close to their tops, but SEE is suppressed by the secondary whiskers. The local angle of incidence on secondary whiskers ranges from 45° to 90° dependent on impact parameter to the primary whisker relative the center of the primary whisker, so we have conservatively assumed that the SEY from the sides is reduced by the worst factor expected for the secondary velvet, one half, $\gamma=\gamma_{tops}+\gamma_{sides}/2+\gamma_{bottom}$.

These results indicate that the SEY from a surface can be suppressed by adding a feathered structure to the surface. Furthermore, we speculate that these results can be generalized to other fractal-like shapes, which consist of surfaces that have been scaled down and tiled onto themselves.

VI. DEPENDENCIES OF THE SEY ON THE FEATHER PARAMETERS

To determine the effect of angles of secondary whiskers on SEY, we performed simulations of the SEY for three

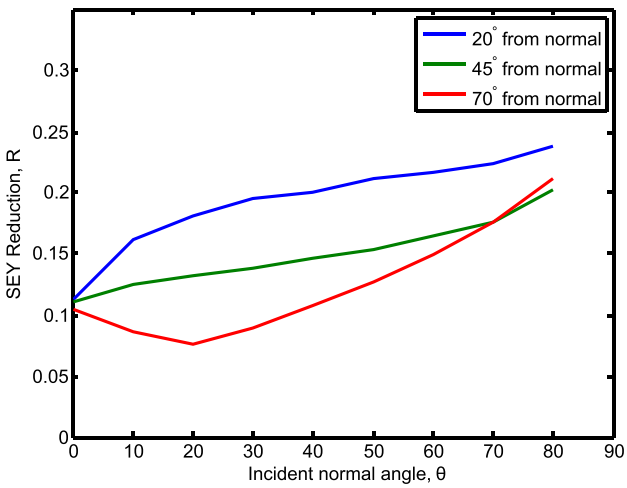

FIG. 3. Curves of SEY reduction factor vs primary angle of incidence for different feathered geometries. These feathers have secondary whiskers at different angles from the normal. Each feather has secondary whiskers pointed farther upward ($+\hat{z}$) than normal, as in Fig. 1.

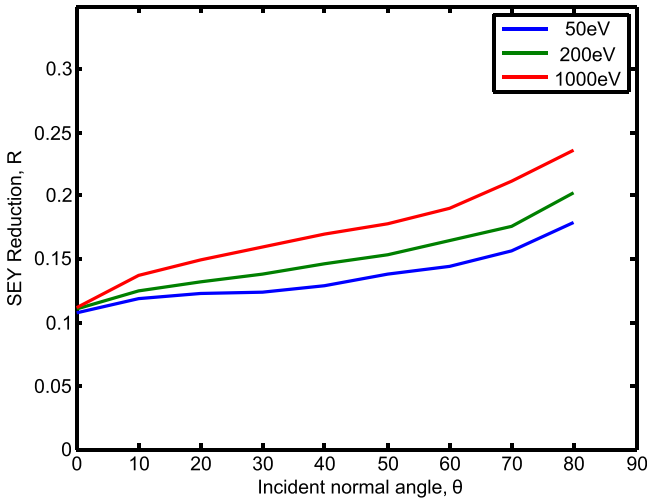

FIG. 4. Curves of SEY reduction factor vs primary angle of incidence for different primary electron energies.

different feather geometries. These feathers had secondary whiskers extending one primary-whisker-radius from the primary whisker surface, so the total effective whisker radius is the same for each case, but different angles from normal to the side of the primary whisker. These SEY curves are depicted in Fig. 3. The 45° case has been already discussed in Sec. VI.

The 20° feather is uniformly less effective at reducing SEY than the 45° feather.

The 70° case shows a very interesting feature: At primary angles of incidence of 20°, this feather suppresses SEY more effectively than the previous case. This can be understood by considering that, at this primary angle of incidence, primary electrons are incident on secondary whiskers almost normally and therefore are maximally suppressed.

We also simulated SEY from the same feather discussed in Sec. VI for three different primary electron energies. The three cases are depicted in Fig. 4. Over a range of energies spanning a factor of 20, we find that the SEY suppression varies less than 30%. This small variation with energy is only due to the change in the number of elastically and inelastically scattered secondary electrons with energy. Elastically scattered secondary electrons produce tertiary electrons elsewhere in the structure.

The feather parameter space left to explore (primary whisker length, radius, and spacing, and secondary whisker length, radius, and spacing) is too large for adequate analysis in this article and is left for follow-up study. We expect that, as with velvet, the SEY reduction will improve with longer and thinner whiskers, but have some irreducible minimum value.[13]

VII. CONCLUSIONS

We simulated and verified that the feathered structures can suppress SEY better than a velvet surface. A velvet surface with one recursion of smaller velvet whiskers grown onto the primary whisker sites looks like a down-feather, and so we refer to such surfaces as "feathered." Such feathered surfaces are suitable for suppressing secondary electrons even for the shallow incident angle of primary electrons. Total SEY reduction factor in the range $R \approx 0.1$ for $\theta \approx 0$ and $R \approx 0.2$ for $\theta \approx 90^\circ$ can be achieved for feathered structure.

ACKNOWLEDGMENTS

The authors would like to thank Yevgeny Raitses, who attracted our attention to the SEY of the velvet. We would also like to thank Eugene Evans, who suggested representing geometry as an isosurface. This work was supported by Air Force Office of Scientific Research.

[1]J. R. M. Vaughan, "Multipactor," IEEE Trans. Electron Devices **35**, 1172–1180 (1988).
[2]Y. Raitses *et al.*, "Effect of secondary electron emission on electron cross-filed current in $E \times B$ discharges," IEEE Trans. Plasma Sci. **39**, 995 (2011).
[3]H. Wang, M. D. Campanell, I. D. Kaganovich, and G. Cai, "Effect of asymmetric secondary emission in bounded low-collisional E×B plasma on sheath and plasma properties," J. Phys. D: Appl. Phys. **47**, 405204 (2014).
[4]Y. Raitses, I. D. Kaganovich, and A. V. Sumant, "Electron emission from nano-and micro-engineered materials relevant to electric propulsion," in *33rd International Electric Propulsion Conference, the George Washington University, Washington, DC, USA* (2013), pp. 6–10.
[5]G. Stupakov and M. Pivi, "Suppression of the effective secondary emission yield for a grooved metal surface," in Proceedings of the 31st ICFA Advanced Beam Dynamics Workshop on Electron-Cloud Effects, Napa, CA, USA, 19–23 April 2004.
[6]L. Wang *et al.*, "Suppression of secondary electron emission using triangular grooved surface in the ILC dipole and Wiggler magnets," in Proceedings of the Particle Accelerator Conference (PAC 2007), Albuquerque, NM, USA, 25–29 June 2007.
[7]M. T. F. Pivi *et al.*, "Sharp reduction of the secondary electron emission yield from grooved surfaces," J. Appl. Phys. **104**, 104904 (2008).
[8]Y. Suetsugu *et al.*, "Experimental studies on grooved surfaces to suppress secondary electron emission," in *Proceedings of the IPAC'10, Kyoto, Japan* (2010), pp. 2021–2023.
[9]D. Ruzic, R. Moore, D. Manos, and S. Cohen, "Secondary electron yields of carbon-coated and polished stainless steel," J. Vac. Sci. Technol. **20**, 1313 (1982).
[10]L. Aguilera *et al.*, "CuO nanowires for inhibiting secondary electron emission," J. Phys. D: Appl. Phys. **46**, 165104 (2013).
[11]R. Cimino *et al.*, "Search for new e-cloud mitigator materials for high intensity particle accelerators," in *Proceedings of the IPAC2014, Dresden, Germany* (2014), pp. 2332–2334.
[12]C. E. Huerta and R. E. Wirz, "Surface geometry effects on secondary electron emission via Monte Carlo modeling," in *52nd AIAA/SAE/ASEE Joint Propulsion Conference* (American Institute of Aeronautics and Astronautics, 2016).
[13]C. Swanson and I. D. Kaganovich, "Modeling of reduced effective secondary electron emission yield from a velvet surface," J. Appl. Phys. **120**(21), 213302 (2016).
[14]M. Patino, Y. Raitses, and R. Wirz, "Secondary electron emission from plasma-generated nanostructured tungsten fuzz," Appl. Phys. Lett. **109**(20), 201602 (2016).
[15]V. Baglin, J. Bojko, O. Grabner, B. Henrist, N. Hilleret, C. Scheuerlein, and M. Taborelli, "The secondary electron yield of technical materials and its variation with surface treatments," in *Proceedings of EPAC 2000, Austria Center, Vienna,* 26–30 June 2000, pp. 217–221.
[16]M. Ye, D. Wang, and Y. He, "Mechanism of total electron emission yield reduction using a micro-porous surface," J. Appl. Phys. **121**(12), 124901 (2017).
[17]H. Von Koch, "Sur une courbe continue sans tangente, obtenue par une construction gomtrique lmentaire," Ark. Mat. **1**, 681704 (1904).
[18]*Vtorichnaya Elektronnaya Emissiya*, edited by I. M. Bronstein and B. S. Fraiman (Nauka Publisher, Moskva, 1969), p. 340 (In Russian).
[19]X. Qin, Z. Miao, Y. Fang, D. Zhang, J. Ma, L. Zhang, Q. Chen, and X. Shao, "Preparation of dendritic nanostructures of silver and their characterization for electroreduction," Langmuir **28**(11), 5218–5226 (2012).
[20]J. Scholtz *et al.*, "Secondary electron emission properties," Phillips J. Res. **50**, 375 (1996).